THE DESIGN OF POLE-PIECES

(The field in an air-gap computed from external sources)

Dave Masters and Denis Midgley
Applied Science and Mathematics Building, Hull University

ABSTRACT

A method is described for the solution of n-dimensional field problems with Dirichlet boundary conditions. Matrices of only (n-1) dimensionality are needed because the field is computed from chosen external sources just outside the boundary. Examples are given of the solution to a two-dimensional Laplace equation, which is relevant to the design of pole-pieces for experiments in an air-gap on a magnetoresistor or similar specimen. It is concluded that the usual 30^{o} tapered convex pole-tip is sometimes inappropriate and that a concave design may be needed.

1. INTRODUCTION

Experiments often require an air-gap, in which the magnetic flux density is to be maximised or, in some instances, is to be made as uniform as possible. Standard electromagnets usually provide a choice of two pole-tips, one flat, the other with a convex taper at the outer edge. The tapered poles are sometimes described as 'flux-concentrators'. This description may fit the case of a maximum flux-density experiment, which is pursued well into saturation. But, it is incorrect, if applied to an electromagnet in the attempt to achieve an assigned, central flux-density from limited ampere-turns in the absence of saturation.

Working with magnetoresistors of small size, Goldsmid[1] does not taper the edges of pole-faces, which are larger than the resistors. He argues that, with or without the taper, the central line of the magnetic field intensity obeys the law of Ampere

$$\oint \underline{H}.\underline{dl} = NI \qquad \ldots\ldots 1)$$

over the same path and, therefore, the same value of H remains at the centre. With no taper the edge-effect is more remote and the central field is more uniform than when the taper is present.

This line of argument may be pursued further. In some magnetoresistor applications, uniformity of the field is less important than concentration of the maximum flux onto the specimen.[2] The present work shows that, quite opposite to the convexity of the usual taper, a concavity is what is required on the pole-face. Figure 1 is an illustration of a rectangular co-ordinate two-dimensional field in an air-gap. At the end of the uniform part of the gap, instead of the usual upward change of direction on the boundary, we make a downward change. The pole-face works like a lens and can be seen to concentrate the field in the required place towards the centre of the image plane.

2. COMPUTATION FROM EXTERNAL SOURCES

A means for computing the potential to satisfy Laplace's equation is required for, in general, three dimensions and curved boundaries subject to known boundary conditions. An attractive method is that of de Mey,[3] who computes the n-dimensional interior field from an (n-1) dimensional array of sources on the boundary. This reduces the matrices by one dimension, but special treatment is needed for the self-terms on the principal diagonal in order to avoid singularities like $\ln(a-r)$ when $r=a$.

We take a somewhat different approach, which imitates nature in the matter of a boundary layer. We specify the potential on the boundary but arrange the sources to be external, displacing them an assigned distance beyond the boundary. Each source begins as an unknown magnetic charge; the field at any point is expressible as the sum of contributions from these charges; the contributions are of the form

$$Q.\ln(a - r) \qquad \ldots\ldots 2)$$

in the case when the sources are chosen to be line-charges; forcing the sum to the boundary value at n selected points generates simultaneous equations in $Q_1, Q_2, Q_3 \ldots Q_n$; solving the equations delivers $Q_1 \ldots Q_n$ as output; the summations can now be performed for any point, allowing the potentials everywhere to be calculated and the equipotentials to be plotted.

For two-dimensional rectangular-coordinate problems it is advantageous to apply the structures of ALGOL68 for the complex potential W. When this is done, the contours defined by RE of W and IM of W become curvilinear squares as illustrated in Fig.1.

3. PLOTTING OF RESULTS

The results have been produced by a routine which draws contours at specified levels for function values given at points on a regular grid.

The algorithm, which is described in detail in Reference No.4 is simple, fast, robust and produces good results. As worse methods exist and are used it may not be inappropriate to outline it.

For each contour level we first mark the edges of each cell of the rectangular grid as being intersected by the contour or not. This can be conveniently done with a bit map. Then starting from some marked edge (initially we choose edges on the boundary and when they have all been used we start from interior edges) we search the adjacent cell for an exit. When an exit edge has been found we move to it (interpolating function values) and repeat the process, unmarking edges as we go, until we meet the boundary or come back to the starting point. (All contour lines are either closed or intersect the boundary twice). We then go to some other starting place and repeat the process until all marks are removed. Sometimes, in the case of a badly behaved contour line, a dead end will be reached but this is no problem: the process is stopped and resumed elsewhere.

The method has the desirable property that it traces a whole contour at one go and behaves well at singular points.

4. CIRCULAR POLE-FACE DESIGN

It is possible to compute the field for realistic circular cylindrical pole-pieces by method of Fourier synthesis, but convergence is not rapid. 5) If the present method is to be applied, then the external sources become elementary rings of equivalent charge. We may also have actual rings of current representing the magnetising turns. Many reference books of electromagnetism offer a solution to the problem of the potential for a charged ring in terms of an infinite series of Legendre functions. We find it neater to adapt an elliptic integral solution described by Moon and Spencer. 6)

If current I flows in a ring of radius a the single-component vector potential $\underline{A}$ at a point r,z is given by

$$\underline{A} = \frac{\mu I a}{2\pi} \int_0^{\pi} \frac{\cos\psi \cdot d\psi}{\sqrt{(r^2+z^2+a^2) - 2ar\cos\psi}} \quad \ldots\ldots 3)$$

where ψ is the angle between r and the radius to an element of the ring.

We introduce complete elliptic integrals K and E of the first and second kinds :

$$K = \int_0^{\pi/2} \frac{dx}{\sqrt{1 - k^2\sin^2 x}} \quad \ldots\ldots 4)$$

$$E = \int_0^{\pi/2} \sqrt{1 - k^2\sin^2 x}\, . dx \ldots\ldots 5)$$

where k is given by :

$$k^2 = \frac{4ar}{(r+a)^2 + z^2} \quad \ldots\ldots 6)$$

A result for $\underline{A}$ in terms of K and E is deduced thus:

$$\underline{A} = \frac{\mu I a k}{2\pi\sqrt{ar}} \left(\frac{2-k^2}{k^2} \int_0^{\pi/2} \frac{dx}{\sqrt{1-k^2\sin^2 x}} - \frac{2}{k^2} \int_0^{\pi/2} \sqrt{1-k^2\sin^2 x}\, . dx \right) \ldots 7)$$

$$\underline{A} = \frac{\mu I}{\pi k}\sqrt{\frac{a}{r}} \left(\left[1 - \frac{k^2}{2}\right] K - E \right) \quad \ldots\ldots 8)$$

by making the change of variable :

$$\psi = \pi + 2x \quad \ldots\ldots 9)$$

For the case of charged rings, this may be adapted to an algorithm for the scalar potential on replacing $\cos\psi$ by unity in equation 3).

In this axisymmetric problem we are denied the convenience of conjugate functions, but the equipotentials can be computed as before. The complete elliptic integrals replace the former logarithmic and hyberbolic functions as the basis for the construction of the resultant field from contributions by each external source.

Results are quite analagous to those of the corresponding two-dimensional rectangular-coordinate problem of Fig.1.

Suppose that a test specimen is to be fitted under the flat central section of the pole-piece. Let it be required that the specimen be subjected to the most uniform field that is attainable by adjusting the angle θ of the tapered section. If there were no taper, we know that the equipotentials turn upwards into the region of the fringe. An angle θ as large as that of Fig.1 is seen to turn these equipotentials downwards. We therefore anticipate that an angle can be found, which will optimise the uniformity of the field, according to a criterion that remains to be chosen.

Such an optimum angle in fact occurs in each particular case, because, in general, this angle is a function of the dimensions of the gap, the radius of the flat part of the pole and the radius of the tapered extension. For the case where the apex is equidistant from the axis, the image plane and the outer edge of the taper section, the optimum angle is found to lie between 11.4° and 11.6° based on a computation from 14 external ring sources; the criterion of uniformity for this case is taken as the constancy of potential along a line midway between the pole flat and the image plane.

5. DISCUSSION

It is found that the offset distance for the boundary layer allows a choice between rapid convergence as n increases (thin layer) and smoothness of the field on the boundary (thick layer).

The shape of the external source may also be chosen. In Figure 2 is shown a) the individual field of a line charge and b) the composite field from a row of such line charges.

On a straight boundary like this, if the solution to the simultaneous equations has shown that adjacent trial line-charges have worked out to be approximately of equal value, then strip-charges may be substituted with advantage.

Figure 3 shows at a) the individual field of a strip-charge and at b) the composite field. The programs which produce the results that are compared in these two Figures differ only in the change of a subroutine from $W = c\ln(z)$ for line sources to $W = \operatorname{arccosh}(z)$ for strip sources.

The strip sources are seen clearly to lead to a smoother field near to the boundary in such a case.

We have shown in Section 4. how the method extends to three dimensions with axial symmetry. Other extensions could be to take account of finite permeability in the magnetic material and to remove the artificiality of permitting only one change of direction to control the fringing flux. It should then become possible to design a curved profile to achieve a specified field in the gap.

A compromise must remain between maximising the flux ($\theta = 90^{\circ}$) but with a severely non-uniform field in the target area and on the other hand achieving a near uniform field ($\theta = c.11^{\circ}$ in one case).

6. REFERENCES

1. Goldsmid, H J. Longitudinal thermomagnetic amplifiers. J. Phys. D. 10 p109 June 1977.
2. Midgley, D. Recent advances in the Hall effect. Advances in Electronics and Electron Physics. 36 Academic Press. 1974.
3. De Mey, G. Integral equation for the potential distribution in a Hall generator. Electronics Letters. 9 p264 June 1973.
4. Cottafara, G and Le Moli, G. C.A.C.M. 12, 7, p386 1969.
5. Midgley, D and Smethurst, S W. Field plotting by Fourier synthesis and digital computation. Proc.IEE. 112, No 10, p1945 October 1965.
6. Moon, P and Spencer, E H. Electrodynamics. Van Nostrand p102 1960.

7. ACKNOWLEDGMENTS

We thank Professor H.J. Goldsmid of the University of Sydney, Australia for inspiring discussions on magnet design, the University of Hull O/C Grants committee for financial assistance and staff of the Computer Centre for help with computation.

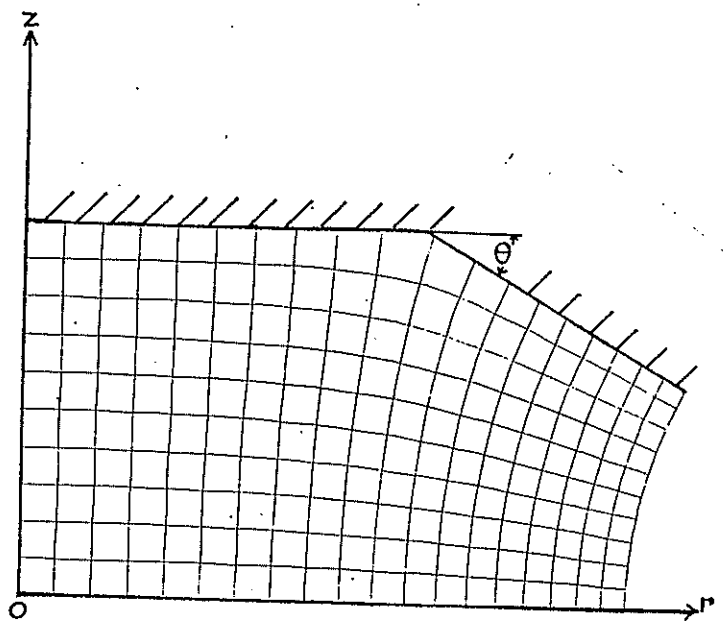

FIG. 1 CONCENTRATION OF FLUX DENSITY UNDER A SHAPED POLE PIECE.

OZ axis

Or image plane

/// magnetic material of indefinitely high permeability

All internal intersections of equipotentials and lines of force are as produced by the computer and graph plotter, for the two-dimensional rectangular co-ordinate case.

(a)

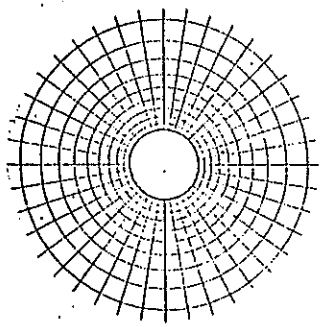

(b)

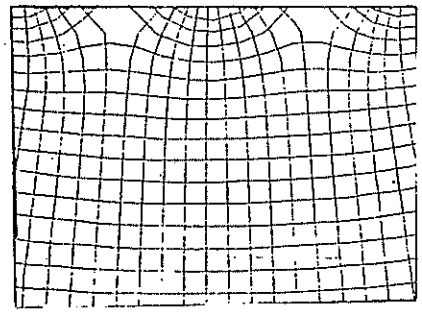

FIG. 2 CONTOURS OF COMPLEX POTENTIAL W = U + jV

(a) For a single line source W = cln(r + jz) where cln denotes the complex logarithmic function.

(b) For 10 line sources near a straight boundary after matrix inversion. The sources are placed outside the boundary, where contours of constant-V would converge if produced.

(a)

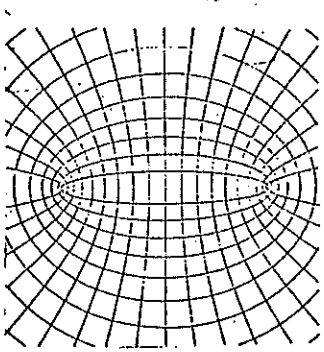

(b)

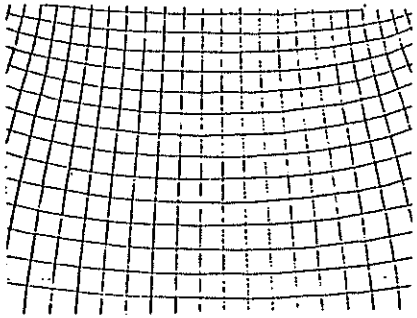

FIG. 3 CONTOURS OF COMPLEX POTENTIAL $W = U + jV$

(a) For a single strip source $W = \text{arccosh}(r + jz)$ where arccosh denotes the complex inverse hyperbolic cosine function.

(b) For 10 strip sources near a straight boundary after matrix inversion. The sources are placed outside the boundary in the same locations as for Fig.2(b).

RESOLUTION DE L'EQUATION DE LAPLACE PAR UNE METHODE DE POTENTIELS AUX LIMITES

M. Jufer et H.J. Remus
Laboratoire d'Electromécanique de l'Ecole Polytechnique Fédérale LAUSANNE (Suisse)

RESUME

La méthode proposée a pour but de résoudre l'équation de Laplace par un algorithme basé sur la distribution du potentiel magnétique associé au pourtour d'un espace fermé. Elle s'applique particulièrement bien au cas d'un entrefer séparant le stator et le rotor d'un moteur à reluctance variable. Elle conduit à une résolution généralement plus rapide que les méthodes de différence finie ou d'éléments finis.

Deux applications sont proposées :

- la première traite de la perméance de deux structures dentées en fonction de leur position relative. Le problème de l'interpolation entre les points calculés est évoqué dans le but d'une diminution des temps de calcul. Une solution par le biais des fonctions Spline fournit les meilleurs résultats.
- la seconde traite du calcul des caractéristiques d'un moteur pas à pas monophasé électromagnétique. L'aimant permanent est remplacé par une source de potentiel magnétique scalaire.

1. INTRODUCTION

La génération d'une force ou d'un couple de nature électromagnétique est toujours associée à une variation des inductances propres ou mutuelles d'un système électromécanique. Pour un tel système comprenant n circuits électriques, la force dans une direction x s'écrit :

$$F_x = \frac{1}{2} \sum_{k=1}^{n} \sum_{p=1}^{n} \frac{\partial L_{kp}}{\partial x} i_k i_p$$

L_{kp} est l'inductance mutuelle entre les circuits k et p.
i_{kp} est le courant du circuit correspondant.

La connaissance des inductances propres ou mutuelles conditionne le calcul des forces. On peut également recourir au tenseur de Maxwell. Dans les deux cas, la résolution de l'équation de Laplace doit s'effectuer dans l'entrefer séparant les parties mobiles. Des méthodes classiques telles que les éléments finis ou les différences finies permettent une résolution. Dans un tel cas, une méthode présentée dans la référence 1 permet une résolution plus rapide à précision égale. Après un bref rappel de la méthode, celle-ci sera appliquée à deux cas particuliers.

2. METHODE DES POTENTIELS AUX LIMITES

Soit un contour fermé sur le pourtour duquel le potentiel scalaire θ est connu. Un certain nombre de points de coordonées (x_n, y_n) sont repérés sur ce pourtour. Les conditions aux limites sont données comme suit pour le point n :

$$a_n \theta_n + b_n \left(\frac{\partial \theta}{\partial t}\right)_n + c_n \left(\frac{\partial \theta}{\partial p}\right)_n = d_n$$

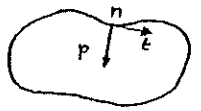

Fig 1

a_n, b_n, c_n, d_n sont des coefficients connus.
t est la composante tangentielle au contour (voir fig. 1).
p est la composante perpendiculaire au contour.
On définit deux fonctions auxiliaires : σ_n et ψ_{mn}. On est alors conduit aux relations :

$$a_m \sum_{n=1}^{N} \sigma_n \psi_{nm} + b_m \sum_{n=1}^{N} \sigma_n \left(\frac{\partial \psi}{\partial t}\right)_{n,m} + c_m \sum_{n=1}^{N} \sigma_n \left(\frac{\partial \psi}{\partial p}\right)_{n,m} = d_n$$

$$\psi_{nm} = \mathrm{Re}\left\{\frac{1}{\underline{t}_n}\left[(\bar{\underline{Z}}_m - \underline{Z}_{n+1}) \ln(\bar{\underline{Z}}_m - \underline{Z}_{n+1}) - (\bar{\underline{Z}}_m - \underline{Z}_n) \ln(\bar{\underline{Z}}_m - \underline{Z}_n) + (\underline{Z}_{n+1} - \underline{Z}_n)(1 + \ln k)\right]\right\}$$

$$\left(\frac{\partial \psi}{\partial p}\right)_{nm} = I_m\left\{\frac{\underline{t}_m}{\underline{t}_n} \ln \frac{\bar{\underline{Z}}_m - \underline{Z}_{n+1}}{\underline{Z}_m - \underline{Z}_n}\right\}$$

$$\left(\frac{\partial \psi}{\partial t}\right)_{nm} = \mathrm{Re}\left\{\frac{\underline{t}_m}{\underline{t}_n} \ln \frac{\bar{\underline{Z}}_m - \underline{Z}_{n+1}}{\underline{Z}_m - \underline{Z}_n}\right\}$$

avec $\underline{Z}_n = x_n + j\, y_n$

$\underline{t}_n$ = expression complexe du vecteur unité tangentiel

$\underline{\bar{Z}}_m = \frac{1}{2}(\underline{Z}_m + Z_{m+1})$

k = constante arbitraire

La résolution du système de N équations ci-dessus permet de déterminer la distribution de l'induction :

Pour la composante tangentielle : $B_{tm} = -\mu_0 \sum_{n=1}^{N} \sigma_n \frac{\partial \psi_{nm}}{\partial t}$

Pour la composante normale : $B_{pm} = -\mu_0 \sum_{n=1}^{N} \sigma_n \frac{\partial \psi_{nm}}{\partial p}$

Il est alors possible de déterminer soit la perméance associée à l'espace étudié, soit la force s'exerçant sur une surface par l'intégrale du tenseur de Maxwell.

3. APPLICATION A UNE STRUCTURE DENTEE

La fig. 2 présente deux structures dentées opposées, typiques d'un moteur pas à pas. Il s'agit de déterminer la perméance en fonction du décalage ε. Le potentiel est constant sur chacune des surfaces opposées. Le calcul a été effectué pour 8 points de décalage. L'interpolation entre ces points, nécessaire pour l'étude d'un comportement dynamique par exemple, peut s'effectuer par une décomposition en série de Fourier. Un tel résultat est donné à la courbe 1 de la fig. 3. La courbe 1 de la fig. 4 correspond à la dérivée de cette fonction en fonction du décalage ε. Elle doit intervenir dans le calcul de la force ou du couple. Celle-ci présente des oscillations sans signification physique, liées au nombre de points de l'approximation. Les courbes 1 des fig. 5 et 6 correspondent respectivement à la perméance et sa dérivée pour une approximation en série de Fourier, associée à 16 points par période. Bien que de moindre amplitude, les anomalies subsistent. Une amélioration importante peut être apportée par une interpolation au moyen de fonctions Spline 2. Celles-ci sont basées sur des polynômes du 3ème degré, définis par tronçon. Cette technique d'interpolation présente plusieurs avantages, parmi lesquels un lissage et un temps de calcul très faible. Les courbes 2 des fig. 3 et 4 présentent les résultats de cette technique, pour 8 points. Les courbes 2 des fig. 5 et 6 sont les grandeurs homologues relatives à 16 points.

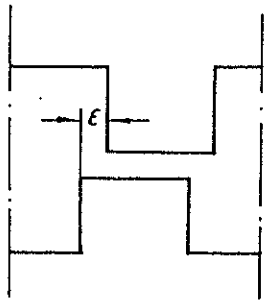

Fig. 2

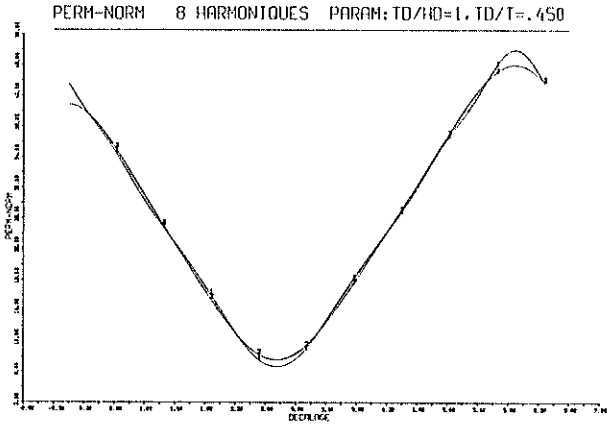

Fig. 3

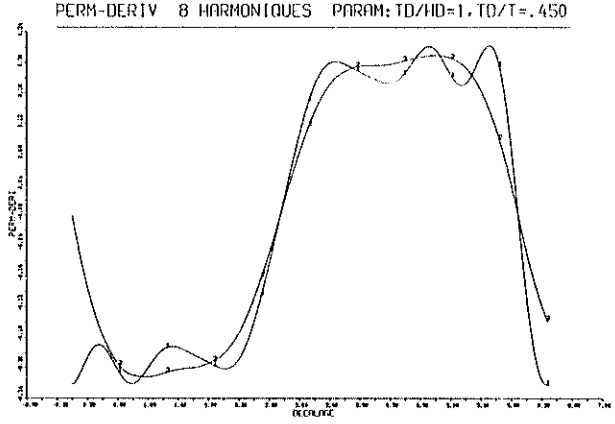

Fig. 4

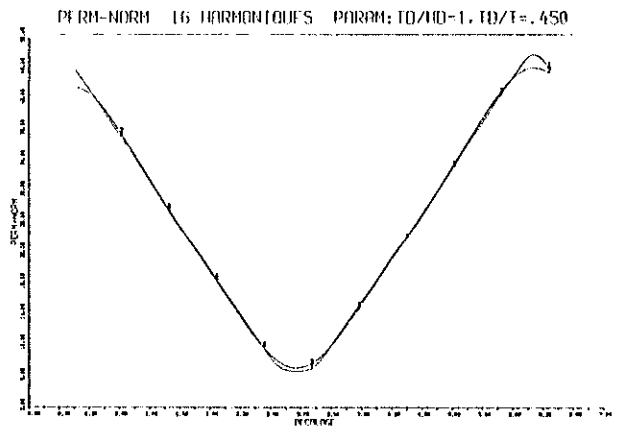

Fig. 5

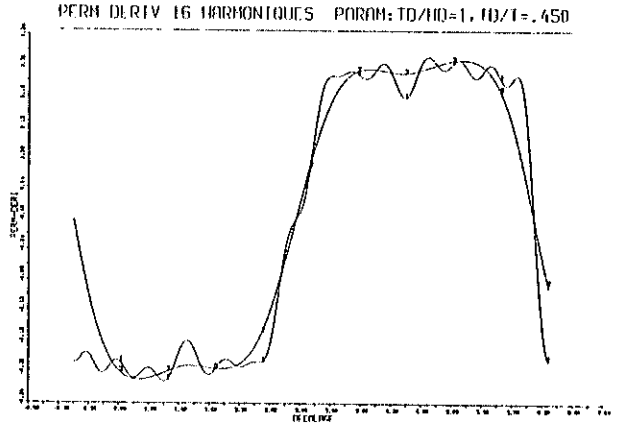

Fig. 6

4. APPLICATION A UN MOTEUR ELECTROMAGNETIQUE MONOPHASE

Les moteurs électromagnétiques, caractérisés par un aimant permanent mobile, sont particulièrement délicats à calculer. A titre d'exemple, le moteur pas à pas monophasé de la fig. 7 sera analysé par la méthode des potentiels aux limites. En première approximation, on admet une distribution sinusoïdale du potentiel magnétique à la surface de l'aimant, conformément à la fig. 8, avec un potentiel nul sur les pôles statoriques excentrés. La fig. 9 présente la caractéristique des couples dû à l'aimant seul (M_a) et mutuel (M_{ab}) en fonction de la position angulaire. La fig.10 illustre la distribution des composantes tangentielle et radiale de l'induction à la périphérie du rotor en position d'équilibre avec courant. La fig. 11 présente les mêmes grandeurs, en position d'équilibre stable, sans courant.

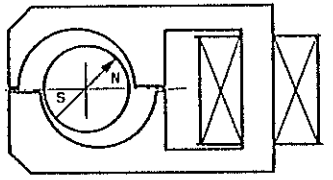

Fig. 7

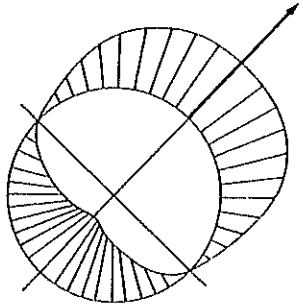

Fig. 8

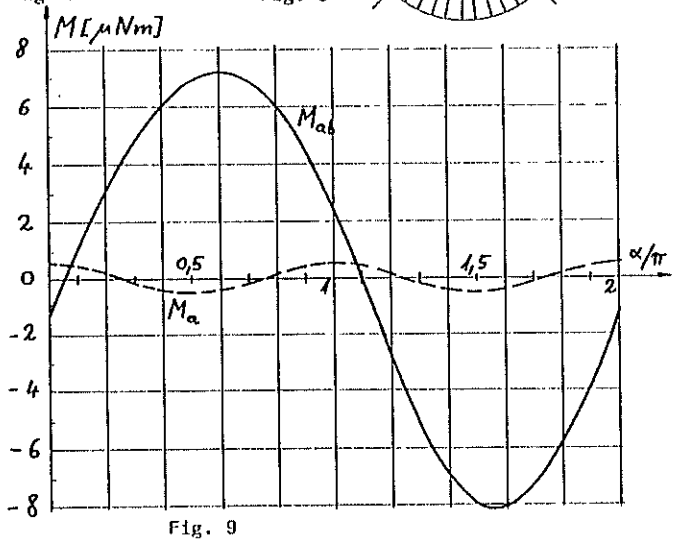

Fig. 9

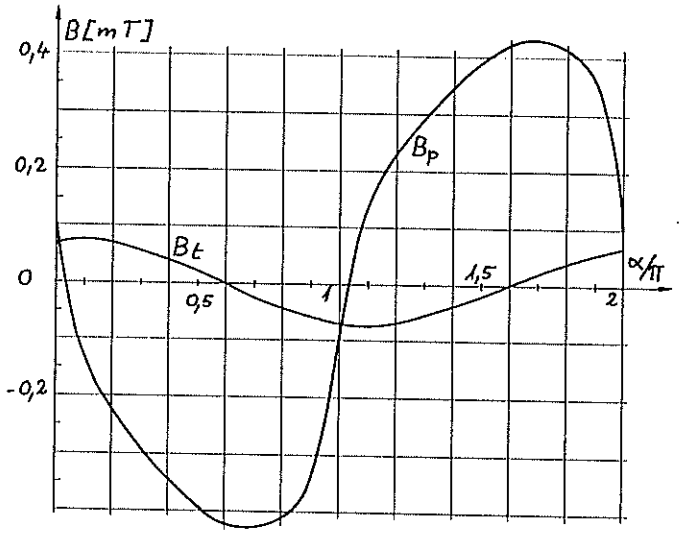

Fig. 10

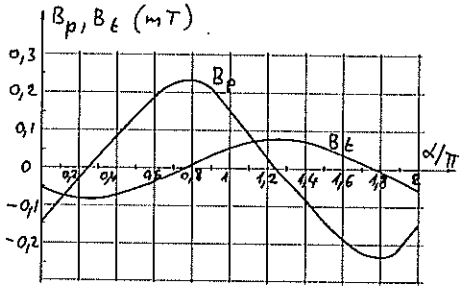

Fig. 11

5. CONCLUSION

La résolution de l'équation de Laplace par la méthode de potentiel aux limites décrite présente un certain nombre d'avantages :

- la résolution est plus rapide, pour de nombreux cas de figures, qu'en recourant à une technique d'éléments finis;
- on obtient directement les principales grandeurs (induction, champ, tenseur de Maxwell, etc.) sur la surface du milieu analysé;
- la précision et la convergence sont généralement bonnes.

En revanche, cette technique ne peut pas s'appliquer à des milieux saturables. Elle implique la connaissance du potentiel sur les surfaces.

6. REFERENCES

1. H.D. Chai, "Technique for finding permeance of toothed structures of arbitrary geometry". Proceedings of the International Conference on Stepping Motors and Systems. University of Leeds, 1976.

2. R. Sauer, I. Szabo, "Mathematische Hilfsmittel des Ingenieurs". Vol. III, pp 265-277, Springer Verlag, 1968.

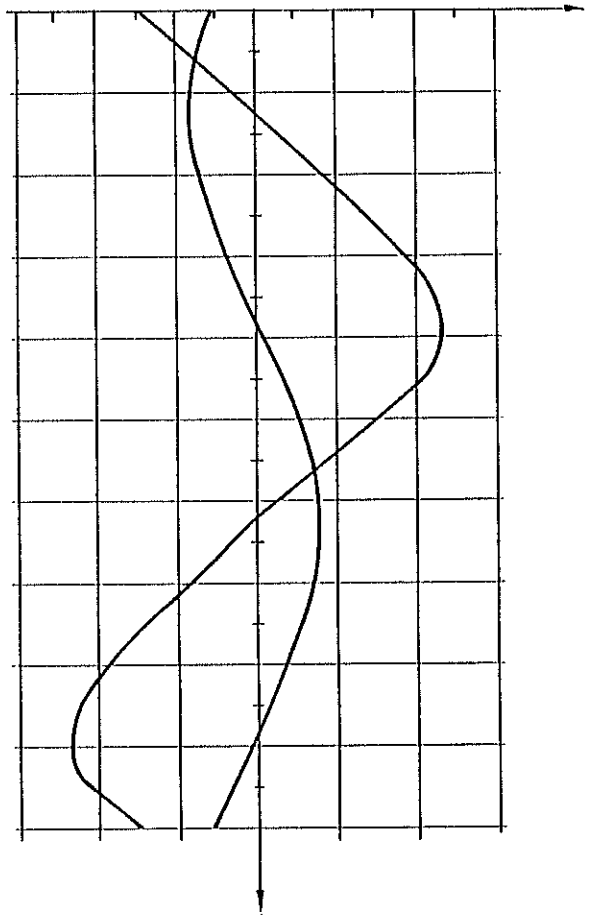

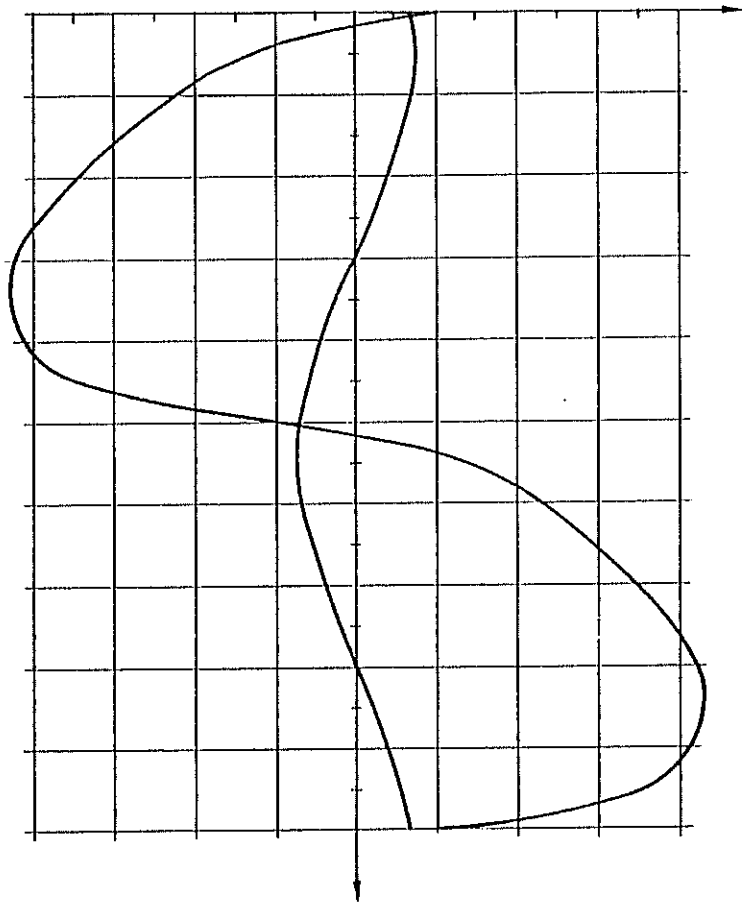

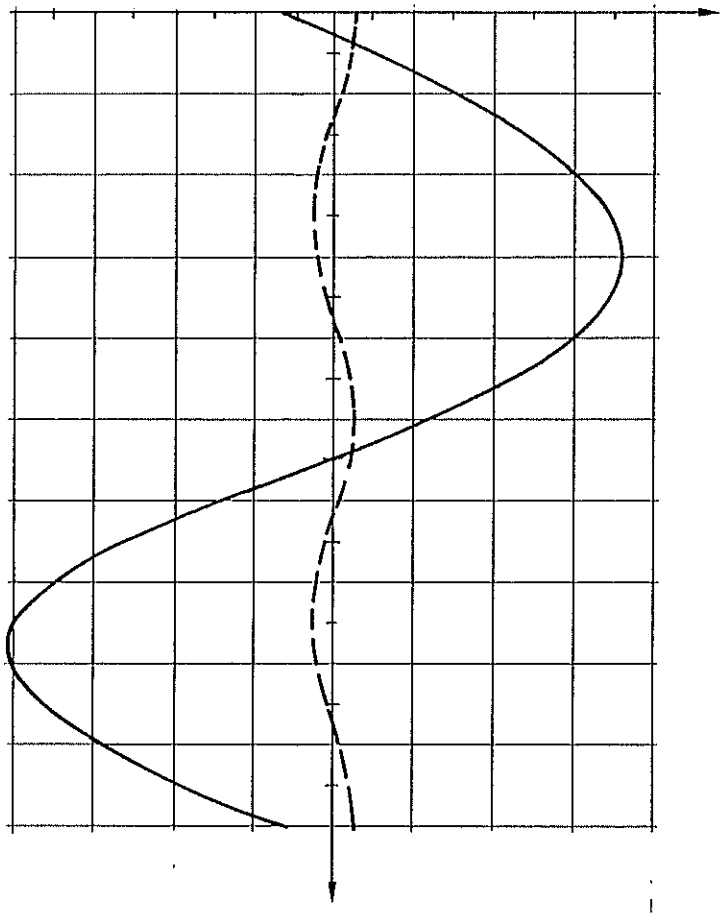

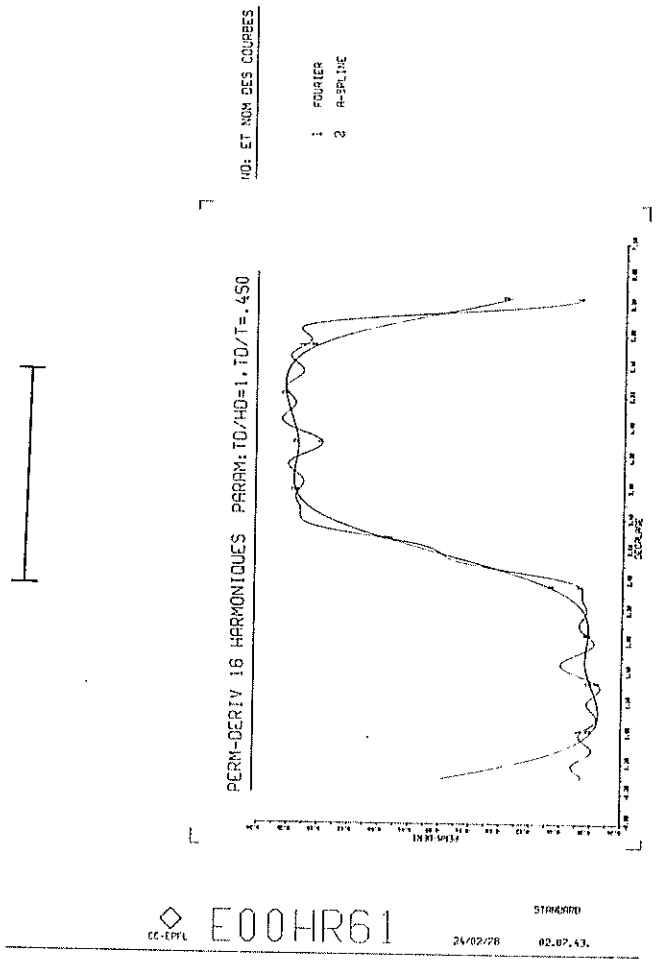

CC-EPFL E00HR61 STANDARD 24/02/78 02.07.43.

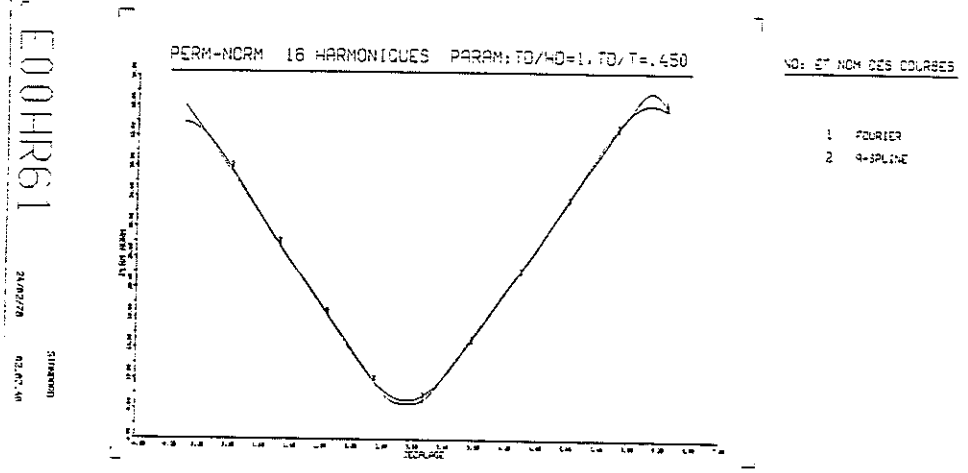
PERM-NORM 16 HARMONIQUES PARAM:TD/HD=1,TD/T=.450
NO: ET NOM DES COURBES
1 FOURIER
2 B-SPLINE

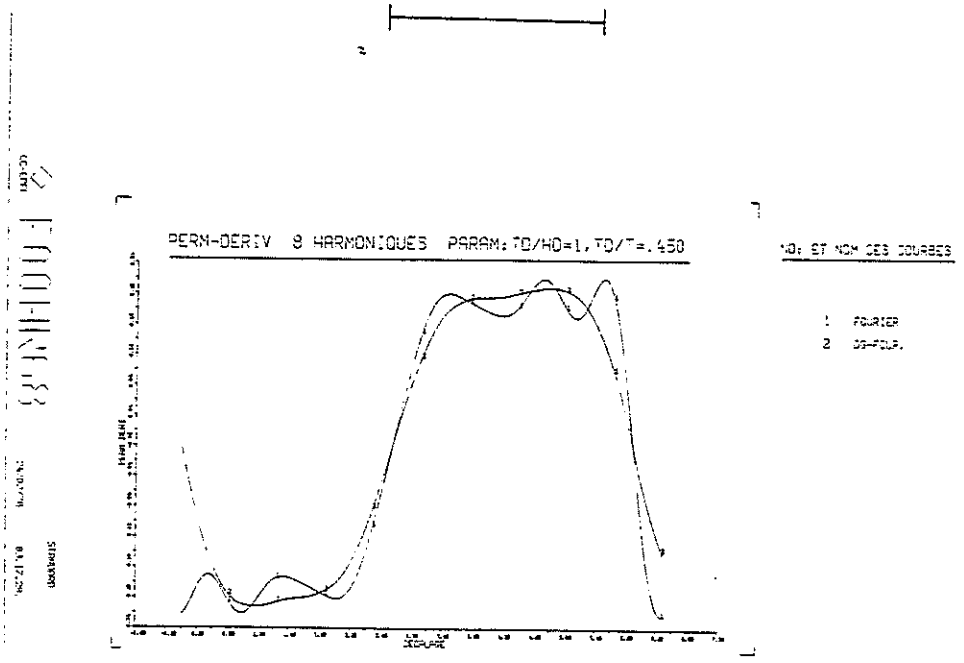
PERM-DERIV 8 HARMONIQUES PARAM:TD/HD=1,TD/T=.450
NO: ET NOM DES COURBES
1 FOURIER
2 DS-POLP.

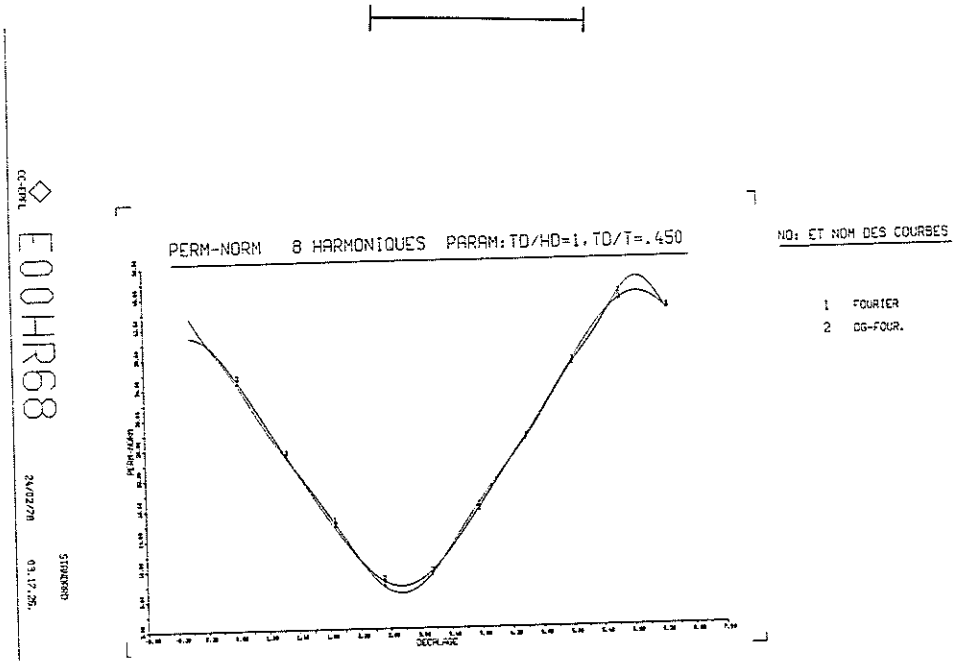
CG-EDF
E00HR68
24/02/70
03.17.20
CHARGEMENT
PERM-NORM 8 HARMONIQUES PARAM:TD/HD=1,TD/T=.450
PERM/NORM
DECALAGE
NO: ET NOM DES COURBES
1 FOURIER
2 DG-FOUR.

FINITE ELEMENT MAGNETIC FIELD CALCULATION TAKING INTO ACCOUNT SATURATION AND HYSTERESIS

E. Bassi(+),(++), A. Gobetti(++) and A. Savini(+)
+ Istituto di Elettrotecnica dell'Università, I-27100 Pavia, Italy
++ Centro di Calcoli Numerici dell'Università, I-27100 Pavia, Italy

ABSTRACT

Based on the finite element method, a program for the calculation of magnetic field is presented. Simplified representations of magnetization characteristics as well as hysteresis loops are introduced. The two-dimensional field region is discretized by rectangular elements, while the applied current vector is supposed to have a single component and to vary alternatively with time. The program is designed for a general incremental solution of the non linear problem. To improve the solution accuracy and also to prevent the development of numerical instabilities, use is made of equilibrium iterations within preselected steps of computation. A simple example is worked out and improvements for the computer program are indicated in order to make it to be more general and comprehensive.

1. INTRODUCTION

Accurate descriptions of both static and dynamic magnetic field problems are of considerable interest to engineers and physicists[1]. Indeed the performances of most of electromagnetic and electromechanical devices strongly depend on magnetic fields. Examples of engineering applications are represented, for instance, by transformers, reactors, magnets and rotating electric machines.
It is well known that the difficulties experienced in simulating fields in magnetic media mainly lie in the presence of saturation, hysteresis, eddy currents and, on occasion, anisotropy. In general, due to such properties and complex geometries only numerical solutions can be attained. In recent years the finite element approach has been successfully applied to solve non linear magnetic field problems. A number of digital computer programs have been developed for magnetostatic problems by suitably simulating saturation and adopting special numerical technique to obtain better rates of convergence and degrees of approximation in the solution[2,3].
On dealing with magnetodynamic problems, attention is commonly devoted to eddy currents, while hysteresis is usually assumed to be negligible. In some cases this is justified, but in other cases the presence of hysteresis is crucial. Among the major effects of hysteresis there are transient phenomena occurring in power systems because of the switching of electromagnetic devices. It is known, in fact, that, for instance, when a transformer or a reactor is disconnected from the supply, residual core flux is established which, in turn, critically affects inrush currents and voltages. There is also a need to account for hysteresis in the prediction of losses and other performances of special electromagnetic machines and devices. Nevertheless, present general-purpose digital simulation programs are commonly inefficient to accomodate the multi-valued non linear relationships necessary to adequately describe hysteresis effects.
This paper attemps to present a finite element approach to the dynamic magnetic field problem solution, by introducing a generalized and simplified model of the multivalued magnetization characteristic and adopting a special numerical technique for resolution.

2. FORMULATION OF THE PROBLEM

A two-dimensional region R containing iron, air and current leading conductors is considered in the x-y plane bounded by curve C. The following main assumptions are introduced:
- the current density vector $J(x,y)$ and the magnetic potential vector $A(x,y)$ have only one component normal to the region and are, in general, time-dependent;
- magnetic media are taken to be isotropic and exhibiting reluctivity $\nu(x,y)$, dependent on magnetic induction; no conducibility is considered, so that eddy currents can be neglected, for simplicity;
- the field is quasi-stationary so that displacement currents are fully disregarded.

It is well known that, under the foregoing assumptions, the magnetic field problem can be described by the following non linear partial differential equation:

$$\frac{\partial}{\partial x}\left(\nu\frac{\partial A}{\partial x}\right) + \frac{\partial}{\partial y}\left(\nu\frac{\partial A}{\partial y}\right) = -J \qquad (1)$$

The boundary conditions to be satisfied by Eq.(1) may be as follows, i.e.: A or $\partial A/\partial n$ is specified on curve C.
It is perhaps worth noting here that, when the cross sec-

tion of axi-simmetric systems is to be considered, the same Eq.(1) holds, after replacing ν with ν/r and A with Ar, where r denotes the radial coordinate.

3. GENERAL APPROACH

Equation (1) can be reformulated in variational terms by minimizing a non linear energy functional. According to the finite element method the field region is discretized into a set of elements and the energy functional minimized with respect to the potential values at each vertex of the mesh of elements. Hence a system of algebraic non linear simultaneous equations is obtained of the matrix form:

$$S(A)\ A = J \qquad (2)$$

where J is the column vector of impressed current densities, A the column vector of unknown potentials, while matrix S, called reluctance matrix, is function of the values of A.
Various methods, based on step-by-step processes, have been experienced in order to solve matrix Eq. (2) which presents variable coefficients [4]; perhaps the most popular and successful is the Newton Raphson method. Due to the very nature of the dynamic analysis involved, an incremental process is in order here, carried out by linearizing Eq. (2) and solving in terms of increments of variables:

$$S_{i-1}(A)\Delta A_i = \Delta J_i \qquad (3)$$

The solution is thus achieved by applying successive increments of J and adjusting, at each step, matrix S which is therefore named incremental matrix. Unfortunately, two serious disadvantages have to be noted. The first concerns the fact that at each step the incremental reluctance matrix must be reformulated and a new solution of Eq. (3) obtained, thereby originating an extremely uneconomical process if small steps of calculation are considered. The second disadvantage is shown in Fig. 1, where the relationship between any two characteristic parameters of the analysis is represented. It is evident that, if at the beginning of each step the tangent matrix is assumed as incremental reluctance matrix, the difference between computed and exact solution increases and considerable errors in the final solution may be recorded, unless very small steps are considered.

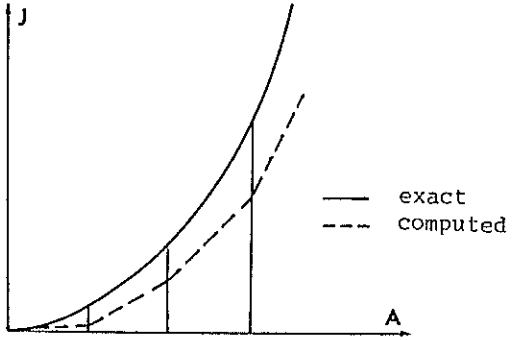

Fig. 1. Comparison of exact and computed relationship between two characteristic parameters of the analysis.

On the contrary, improvements in the overall economy and accuracy of the solution can be attained by suitable modification of the above method (modified Newton Raphson method). In fact, it is possible to bring up the solution to the correct level, whenever the difference between the two curves of Fig. 1 exceeds a prescribed value, by evaluating and redistributing "residual current densities" and then performing equilibrium iterations within each step at constant J and so at constant incremental reluctance matrix. Clearly, as the convergence of these last iterations is rather slow, a judicious combination of both variable and constant incremental matrix process is to be accomplished.
The above two methods have been already widely used in structural finite element analysis, where they are referred to as "variable stiffness method" and "initial stress method" respectively.

4. MATERIAL CONSTITUTIVE RELATION

For purpose of finite element analysis it is necessary to define, for all the materials considered, a constitutive relation between magnetic induction B and field strength H. Unfortunately several difficulties arise for ferromagnetic materials owing to saturation and hysteresis. In fact, also if hysteresis is disregarded, a sin-

gle-valued strongly non linear relation must be considered; so much greater difficulties are encountered when hysteresis is accounted for, because a multi-valued relation is to be assumed. In both cases, of course, a numerical model of the constitutive relation is to be found which must be mathematically simple to reduce computation time but, on the other hand, reasonably close to the actual natural characteristic [5]. In what follows a piecewise linear relationship between B and H is assumed. In particular, as regards hysteresis [6], a simple bi-linear anolonomic model is adopted as shown in Fig. 2.

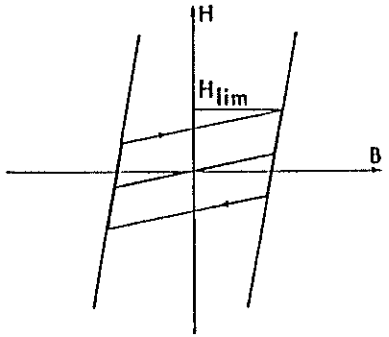

Fig. 2. Typical ferromagnetic material constitutive relation.

The above model may appear rather coarse and ineffective; its great advantage, however, is simplicity since, in this way, the state of material in any condition is completely defined by the knowledge of two parameters only, that is the slope of the characteristic in the point and the updated value of H_{lim}. Obviously, more complicated models can be dealt with, resulting, however, in laborious or even prohibitive implementation task.
The constitutive relation plays an important role in the process of solution. In fact, at each prescribed step of computation, the control of the observance of the constitutive relation is to be accomplished in a finite number of points inside the elements, dependent on the degree of complexity of the shape functions assumed. According to the state of the point, i.e. whether or not violations in the constitutive relation have occurred with respect to the previous step and what they amounted to, reluctance matrix or residual current densities are calculated.

5. COMPUTER PROGRAM

Based on the finite element method, which has long proved to be a very effective discretization procedure, a general computer program for magnetic field solution in the presence of saturation and hysteresis has been developed. Because of the particular problems involved, choice has been made not to modify established programs for linear analysis but to develop a program especially designed for the incremental analysis of non linear problems. The objective has been to have an efficient, modular and easily modifiable program. The main features of such computer program are summarized below. To obtain maximum program capacity the finite elements are arranged in distinct blocks according to their type and whether they are linear or non linear elements. Therefore only the non linear portion of the complete system reluctance matrix is reformed, whilst the linear portion is saved and reinstated when the complete matrix is calculated. To increase the solution efficiency it is allowed to preselect an interval of time steps in which a new reluctance matrix is to be formed and an interval in which equilibrium iterations are to be carried out. Finally, to further minimize the computational time an overlay structure is attributed to the program, so that an optimum high speed storage is obtained.
As mentioned above, the program is devoloped on instantaneous basis by assuming current densities to be anyhow functions of time and performing incremental analysis. The program normally calculates magnetic vector potentials and magnetic inductions and produces output data in printed or plotted formats, as required. The input data consist of nodal point coordinates, boundary condition codes, concentrated nodal point current densities, output options desired and program termination parameters. Element data usually are automatically generated.
The computer program iteratively solves the non linear Eq. (2) by the process which is shortly reported as follows in the case of bi-linear constitutive law.
For each time interval the reluctance matrix is generated, updating the previous one if necessary, and then Gauss-triangularized; next, linearized Eq. (3) is solved and magnetic induction increments as well as field strength increments are evaluated. After the total field strength H is calculated, a test of the constitutive relation is performed. If $H<H_{lim}$, saturation is not reached and a new time interval is considered; otherwise the situation at the previous step must be examined. If saturation has

already been reached, all the increments in field strength must change in order to satisfy the requirements of the new slope of the constitutive relation; if not, only a proper part of the increments must undergo the aforesaid process. In both cases, before applying a new time interval, iterations at constant J are performed, until equilibrium conditions as well as constitutive law requirements are simultaneously satisfied.
The whole process, on time basis, is repeated until a termination condition occurs.
The sequence of computations of the step-by-step solution, in outline form, is represented in Fig. 3.

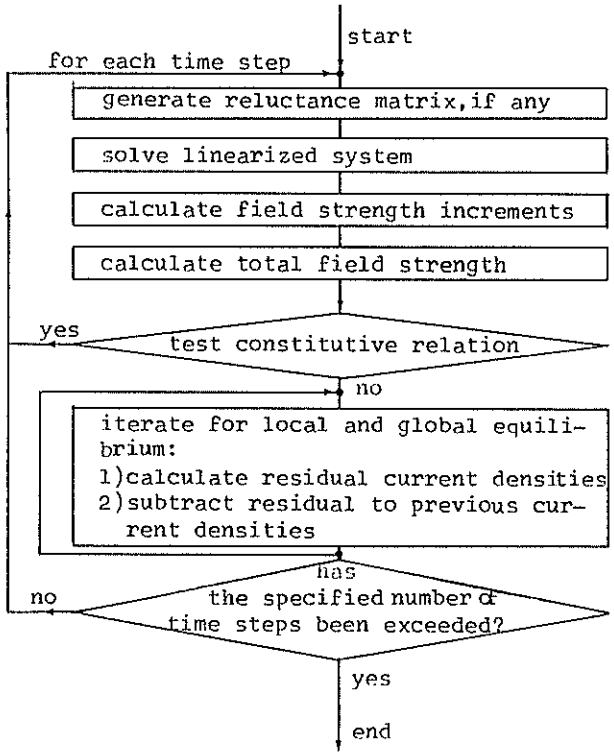

Fig. 3.Flow chart of the step-by-step solution of magnetic field in the presence of hysteresis.

6. APPLICATION

Numerical results have been first obtained by the developed method for certain problems for which solutions by other methods were, to some extent, available. A simple illustrative example of application has been taken, which is shown in Fig. 4. It represents the cross section of the core and the window of a reactor or a transformer in a single-phase unit. Use of simmetry is made to reduce the size of the problem. The region is subdivided in rectangular elements and is subjected to the following specified boundary conditions: i.e. $A = 0$ in ABCD and $\partial A/\partial n = 0$ in AD. Marked dots indicate points where current densities are applied.

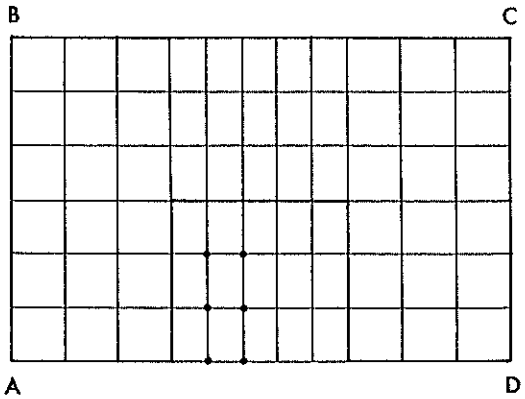

Fig. 4. Finite element mesh for the cross section of a transformer.

Firstly, a magnetostatic analysis has been performed, assuming for iron a single-valued constitutive law coincident with the normal magnetization curve of the material and applying current densities increasing with time in order to reach saturation. To judge the accuracy and efficiency of the new method, the numerical results thus obtained have been compared with those obtained by an available program, based on a different method of solution and suited to solve both linear and non linear problems. Good agreement has been remarked together with some reduction in computer execution time and particularly storage requirement in the case of the present program.
Lastly, a magnetodynamic problem has been considered, as-

suming for iron the multi-valued constitutive law represented in Fig. 2 and allowing current density alternatively to increase and decrease with time linearly.
The waveforms of the principal variables and the values of losses have been readily determined. Each hysteresis cycle has been subdivided into 80 steps of computation. The numerical solution has given fast convergence with no trace of numerical instabilities. The convergence of iterations has been measured in terms of the relative variation in the Euclidean norm of the potential vector of two successive steps; iterations ended when such value became less than 0.001. The calculation has required approximately 8 s for step on a Honeywell 6030 computer and a core storage of about 30 k words using simple precision. The degree of accuracy of the numerical results obtained from the described simulation is presently being examined by means of a comparison with experimental results.
It is believed that,although the above example have simple geometry and a simplified constitutive relation, however, due to the well-established generality of the method, no restrictions practically need to be imposed on geometries and material properties.

7. CONCLUSION

The development of numerical methods in non linear analysis has enabled a more accurate and complete simulation of the magnetic behaviour in ferromagnetic devices to be carried out. In the paper a finite element approach to the magnetic field calculation is described, taking into account saturation and hysteresis. A computer program is presented which is workable for many practical problems and provides a tool to study dynamic systems containing ferromagnetic hysteresis elements.
A model of the magnetization curve and the saturation loop is introduced that is somewhat a comprise between conciseness and accuracy; in any case, it can be readily and efficently implemented on a digital computer. Clearly, more sophisticated models can be dealt with, at the expense of greater implementation effort and additional computational time.
The program is designed for a general incremental solution of non linear problems; so, in particular, it is easily modifiable to extend the analysis by taking account of other phenomena such as eddy currents and non isotropic properties of materials, thereby obtaining a more comprehensive approach to the simulation of ferromagnetic devices.

8. REFERENCES

1. Colonias, J. S. Calculation of Magnetic Fields for Engineering Devices. IEEE Trans. on Mag. vol. 12, 1030-1035, November 1976.

2. Silvester, P. and Chari, M. V. K. Finite Element Solution of Saturable Magnetic Field Problems. IEEE Trans. on PAS, vol. 89, 1642-1651, September-October 1970.

3. Degli Esposti, G., Gobetti, A. and Savini, A. Un Programma per lo Studio di Campi Elettrici e Magnetici Stazionari Basato sul Metodo degli Elementi Finiti. Atti dell'Istituto di Elettrotecnica dell'Università di Pavia, n. 23, May 1976 (internal report).

4. Zienkiewicz, O. C. The Finite Element Method in Engineering Science. Mc Graw Hill, 1971.

5. Hay, J. L. and Chaplin, R. I. Dynamic Simulation of Ferromagnetic Hysteretic Behaviour by Digital Computer. Simulation, vol. 25, 185-191, December 1975.

6. Callegari, C. Estensione di un Programma Incrementale a Modelli Non Lineari Anolonomi. Rapporto dell'Istituto di Scienza delle Costruzioni dell'Università di Pavia, n. 24 (internal report).

PERMANENT MAGNET THREE DIMENSIONAL FIELD COMPUTATION BY CURVILINEAR FINITE ELEMENTS

RAFINEJAD P., COULOMB J.L., MEUNIER G.

Laboratoire d'Electrotechnique de GRENOBLE - E.R.A. 534

BP. 46 38402 SAINT MARTIN D'HERES , FRANCE

A B S T R A C T

Based on the variational formulation of the magnetostatic problems, general three dimensional Finite Element method is implemented. The resulting algorithms includ the tensor expression of the permeability to deal with any anisotropy phenomena. The performance of these algorithms is evaluated through comparison with the analytical results obtained for the example of a cylindrical permanent magnet bounded by a magnetic shielding cylinder. The full application to the design of a permanent magnet device is presented.

I - INTRODUCTION

Dans l'application des méthodes numériques au calcul des champs tridimensionnels, le traitement d'un potentiel scalaire présente un intérêt capital. Ceci aussi bien pour les problèmes de l'électrostatique ou de la magnétostatique des aimants que pour le cas général de calcul de champ magnétique où la définition de tels potentiels réduit l'importance des coûts d'application. En outre, le calcul de ce potentiel scalaire est le résultat d'une extension directe de la méthode des éléments finis bidimensionnelle.

Dans cet article nous rappelons la formulation variationnelle de ce problème et nous présentons la modélisation en éléments finis tridimensionnels curvilignes correspondante.

II - ANALYSE DU CHAMP PAR UNE FONCTION SCALAIRE

La partie d'un système électromagnétique dépourvue de courant de conduction est entièrement caractérisée par un potentiel scalaire ψ choisi tel que :

$$H = \text{grad } \psi \qquad (1)$$

La fonction ψ doit vérifier la conservation du flux (div B = 0) et les conditions aux limites imposées par les domaines voisins. La forme variationnelle de ce problème peut être déduite directement par la condition d'équilibre énergétique du système étudié :

$$\delta L = \int_V \vec{B} \cdot \delta\vec{H} \, dv - \int_S B_n \, \delta\psi \, ds = 0 \qquad (2)$$

où B_n, la composante de l'induction normale à la surface, dépend du champ extérieur. Dans cette expression, le premier terme correspond à la variation de la coénergie magnétique du système et le deuxième indique l'échange énergétique à travers les surfaces extérieures. Cette formulation reste valable quel que soit la relation constitutive entre B et H définie par les propriétés des matériaux.

Dans le cas de la formule générale de l'anisotropie (réf. 1, 2, 3) nous pouvons définir l'expression ci-dessous :

$$B_\Lambda = \mu_o \left| M_o + (1+\chi) H_\Lambda \right| = B_r + \mu_r \mu_o H_\Lambda \qquad (3)$$

où μ_r est connu sous forme d'un tenseur selon les axes de l'aniso-

tropie. Ce que nous écrivons :

$$B = J_A B_r + \mu_o J_A \mu_r J_A^{-1} H = B_r' + \mu_o \mu_r' H \qquad (4)$$

où J_A est la matrice de rotation entre les axes de l'anisotropie et le référentiel global.

La forme explicite de la formulation variationnelle (2) devient :

$$\int_\Omega (\mu_o \mu_r' \text{grad}\psi . \text{grad}\delta\psi + B_r' \text{grad}\delta\psi)\, d\Omega$$

$$- \int_S B_n \delta\psi \, dS = 0 \qquad (5)$$

III - MODÉLISATION EN ÉLÉMENTS FINIS CURVILIGNES

Dans un système de coordonnées locales (u^1, u^2, u^3) toute fonction scalaire ψ ainsi que les coordonnées réelles (x^1, x^2, x^3) (réf. 4) sont interpolées dans un cube de dimensions (2x2x2) par les polynômes de Lagrange α_i :

$$\psi = \sum_{i=1}^{N} \alpha_i (u^1, u^2, u^3)\, \psi_i \qquad (6)$$

$$x^\ell = \sum_{i=1}^{N} \alpha_i (u^1, u^2, u^3)\, X_i^\ell \; ; \; \ell = 1,2,3 \qquad (7)$$

où l'indice i porte sur les N points des coordonnées de Lagrange du cube.

La matrice jacobienne g de transformation s'écrit alors :

$$g_{k\ell} = \frac{\partial x^\ell}{\partial u^k} = \sum^{N} \frac{\partial \alpha_i}{\partial u^k} X_i^\ell \qquad (8)$$

L'expression du champ H d'après les relations (1) et (6) devient :

$$H = \sum^{N} g^{-1} \text{grad}\alpha_i . \psi_i = \sum^{N} C_i \psi_i \qquad (9)$$

Dans le cas des éléments curvilignes, l'utilisation des simplexes complets, ici les cubes à 27 noeuds, est la source de difficultés importantes liées au choix des points intérieur de l'élément. En effet, le choix de ces points a une grande influence sur la précision d'interpolation de la fonction et la régularité de la matrice Jacobienne de transformation, de plus la présence des ces points ou ceux situés sur les côtés rectilignes impose l'addition d'un nombre considérable de données qui ne sont pas significatives du découpage.

Les simplexes non complets possèdent par définition un nombre de points d'interpolation quelconque qui correspondent toujours aux abcisses de Lagrange. Les nouveaux polynômes d'interpolation ß s'obtiennent à partir des anciens en enlevant les points en exédent (réf. 5).

Soit un élément à (N+1) noeuds pour lesquels nous avons défini les polynômes α_i. Toute fonction ψ peut sur cet élément être interpolée par :

$$\psi = \sum_{i=1}^{N+1} \alpha_i \psi_i$$

Si l'on désire retirer le point k de cet élément on peut démontrer que pour toute relation linéaire telle que :

$$\psi_k = \sum_{\substack{j=1 \\ j \neq k}}^{N} d_j \psi_j \qquad \text{avec } \Sigma\, d_j = 1$$

Les polynômes β_j construits à partir des polynômes α_i suivant la formule :

$$\beta_j = \alpha_j + d_j \alpha_k$$

sont des polynômes d'interpolation. On démontre en outre qu'il existe une seule combinaison des paramètres d_j qui rend le dégré des polynômes β_j minimal. Si le point k est situé sur le côté de l'élément les paramètre d_j sont les coefficients du polynôme de Lagrange écrits pour les points qui définissent ce côté et sont égaux à zéro pour

les autres points.

Pour les points situés à l'intérieur, le nombre des paramètres peut être réduit car pour les points j et n dans le simplexe qui sont à la même distance du point k, on aura $d_j = d_n$. On achèvera la détermination des d_j en annulant les coefficients des termes de plus haut degré des polynômes β_j.

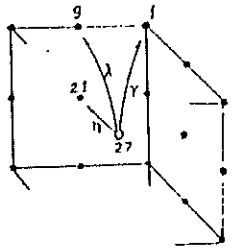

Exemple :

$d_i = \gamma \qquad i = 1,8$

$d_{i+8} = \lambda \qquad i = 1,12$

$d_{i+20} = \eta \qquad i = 1,6$

$\beta_1 = (\frac{1}{8} - \gamma)\, u^2 v^2 w^2 + \ldots$

$\beta_9 = -(\frac{1}{4} + \lambda)\, u^2 v^2 w^2 + \ldots$

$\beta_{21} = (\frac{1}{2} - \eta)\, u^2 v^2 w^2 + \ldots$

d'où : $\gamma = \frac{1}{8}, \quad \gamma = -\frac{1}{4}, \quad \eta = \frac{1}{2}$ vérifiant $\Sigma\, d_i = 1$

Nous avons alors :

$$\beta_1 = \frac{1}{8}(1+u)(1+v)(1+w)(1-w+uv+vw+wu)$$

$$\beta_9 = \frac{1}{4}(1-u^2)(1+v)(1+w)(v+w-1)$$

$$\beta_{21} = \frac{1}{2}(1-u^2)(1-v^2)(1+w)$$

L'optimisation de la fonctionnelle de coénergie aboutit finalement à la relation matricielle suivante relative à un élément :

$$\delta L^e(\delta\psi_i) = |(S^e)\ \{\psi\} + \{P^e\}|\ \delta\psi_i \ , \quad i=1,2\ldots,N \qquad (10)$$

où $|S^e|$ est une matrice carrée de coefficients.

$$S_{ij} = \int_{-1}^{1}\int_{-1}^{1}\int_{-1}^{1} \mu_o(\mu_r' C_i)\ C_j/g/\ du^1 du^2 du^3 \qquad (11)$$

et $\{P^e\}$ un vecteur de composantes

$$P_i = \int_{-1}^{1}\int_{-1}^{1}\int_{-1}^{1} B_r'\ C_i/g/\ du^1 du^2 du^3 - \int_{-1}^{1}\int_{-1}^{1} \vec{B}.\ \vec{U}\times\vec{V}\ du^1 du^2 \qquad (12)$$

L'application d'une formule d'intégration numérique de GAUSS conduit à remplacer l'intégrale par une expression algébrique de la forme :

$$I = \sum_{i=1}^{m}\sum_{j=1}^{n}\sum_{k=1}^{P} w_i\, w_j\, w_k\, f(u_i^1,\ u_j^2,\ u_k^3) \qquad (13)$$

où m, n et P sont les nombres de points d'intégration choisis et w_i, w_j et w_k sont les poids de la formules d'intégration.

Après assemblage sur l'ensemble des éléments, on obtient un système matriciel linéaire ou non linéaire suivant les caractéristiques des matériaux.

IV - TEST DES ALGORITHMES

Nous avons traité à titre de test, le problème d'un aimant cylindrique centré dans un blindage également cylindrique (fig. 1), l'ensemble étant supposé infiniment long. Nous avons comparé une solution analytique avec les résultats obtenus au cours des deux résolutions numériques suivantes :

1°) Traitement bidimensionnel suivant le découpage de la figure 2.

2°) Traitement tridimensionnel avec un découpage en 3 éléments curvilignes de 27 noeuds (fig. 3). La longueur infinie du système a été traduite par une condition de Neumann homogène sur les deux sections du cylindre.

Le tableau 1 réunit l'ensemble de ces résultats.

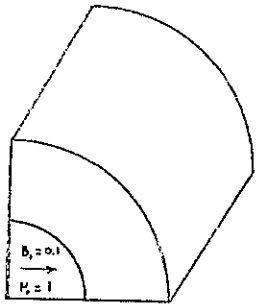

Fig. 1 Aimant et son blindage.

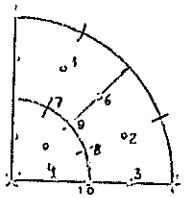

Fig. 2 Discrétisation bidimensionnelle.

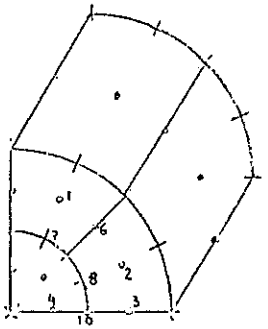

Fig. 3 Discrétisation tridimensionnelle.

Point N°	r	θ	Théorie	2D	3D
1	1.5	67°.5	.445 10^4	.445 10^4	.446 10^4
2	1.5	22°.5	.107 10^5	.108 10^5	.108 10^5
3	1.5	0°	.116 10^5	.116 10^5	.116 10^5
4	0.5	0°	.149 10^5	.149 10^5	.149 10^5
6	1.5	45°	.821 10^4	.823 10^4	.822 10^4
7	1.0	67°.5	.114 10^5	.113 10^5	.114 10^5
8	1.0	22°.5	.276 10^5	.275 10^5	.275 10^5
9	1.0	45°	.211 10^5	.211 10^5	.210 10^5
10	1.0	0°	.298 10^5	.296 10^5	.298 10^5

Tableau 1. Comparaison entre les valeurs théoriques et les résultats numériques obtenus en 2D et 3D.

V - MODÉLISATION D'UN DISPOSITIF À AIMANT PERMANENT

Nous avons utilisé cette méthode pour la modélisation d'un dispositif composé de 4 aimants permanents de forme cubique et d'un cylindre de ferrite logés dans un blindage de forme complexe (fig. 4).

Il est particulièrement intéressant d'appréhender la répartition des lignes de forces du champ magnétique ainsi que sa modification en fonction des variables géométriques des différents composants. D'autre part, il est souhaitable de connaître avec précision l'état de polarisation du barreau de ferrite.

Compte tenu de la géométrie de cet objet, il s'agit ici d'un problème tridimensionnel. Nous avons modélisé ce problème à l'aide de 44 éléments curvilignes à 6 faces et 27 noeuds, ce qui nous donne 540 points (fig. 5). L'affectation de condition de Dirichlet homogène sur le blindage a pour conséquence de réduire le nombre des variables inconnues à 380. Les temps de calcul sur un IBM 360/67 pour l'intégration numérique à 125 points par éléments et la résolution du système linéaire correspondant, sont respectivement de 4 à 10 mn.

La figure 6 représente la visualisation des résultats par un tracé d'équipotentielles sur différentes sections. La figure 7 montre la variation de la polarisation à l'intérieur du barreau de ferrite.

VI - CONCLUSION

Dans cet article, nous avons présenté une application de la méthode des éléments finis tridimensionnels curvilignes au calcul du champ magnétique. Cet exemple met en évidence la nécessité d'un calcul tridimensionnel dont la valeur des résultats justifie le coût de l'opération.

L'utilisation des éléments isoparamétriques a apporté une très grande souplesse d'exploitation ainsi qu'une grande précision

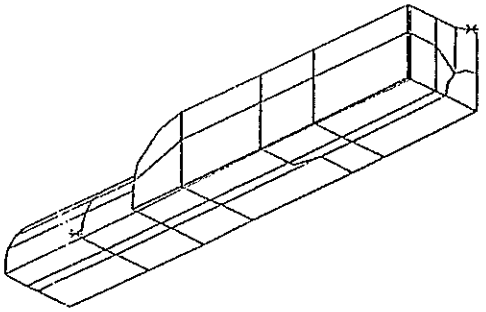

Fig. 5 Modélisation en éléments finis curvilignes

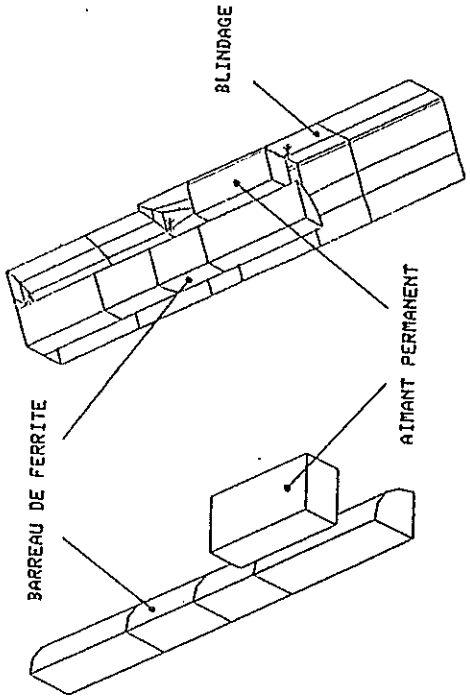

Fig. 4 Vue des 1/8 du dispositif

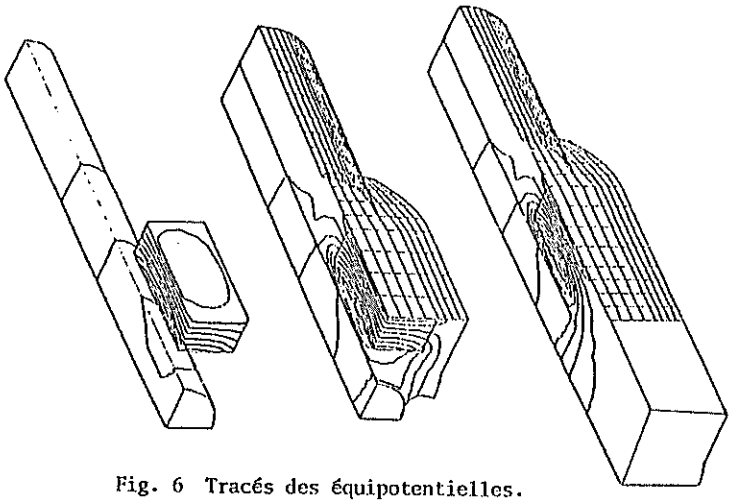

Fig. 6 Tracés des équipotentielles.

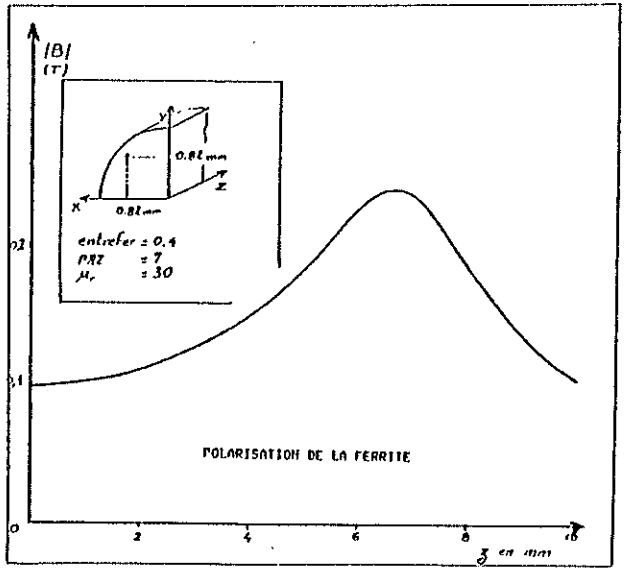

Fig. 7 Polarisation du barreau de ferrite

des résultats. Formulation générale des éléments simplexes dans les systèmes de coordonnées locales, construction dynamique des polynômes d'interpolation, simplicité d'intégration numérique ont permis la réalisation de programmes généraux.

REMERCIEMENTS

Nous tenons à remercier la Société Anonyme des Télécommunications, pour nous avoir confié un problème industriel tridimensionnel.

REFERENCES

1 KAMMINGA W. Finite element solutions for devices with permanent magnets. J. Phys. D: Appl. Phys., Vol. 8, 1975.

2 ZIJLSTRA H. Permanent magnets in magnetic field calculations. Proceedings of COMPUMAG conference, OXFORD 1976, pp. 164-167.

3 POLAK S.J., WACHTERS A., DE BEER A. An account for the use of the FEM for magnetostatic problems. Proceeding of COMPUMAG conference, OXFORD 1976.

4 RAFINEJAD P., COULOMB J.L., Interactive computer techniques in three dimensional modelisation of field problems by finite element method. Proceeding of COMPUMAG conference, GRENOBLE 1978, paper 4.5.

5 RAFINEJAD P. Adaptation de la méthode des éléments finis à la modélisation des systèmes électromécaniques de conversion d'énergie. Thèse de Doctorat d'Etat ès-Sciences GRENOBLE, Janvier 1977.